Published in Journal of Quantitative Spectroscopy and Radiative Transfer, 1972, Vol 12, Iss 5 P 857-872
Archived in Dspace@nitr, http://dspace.nitrkl.ac.in/dspace

LINE SHAPE PARAMETERS FOR HCl AND HF IN A CO_2 ATMOSPHERE*

P. VARANASI, S. K. SARANGI and G. D. T. TEJWANI†

Department of Mechanics, State University of New York, Stony Brook, N.Y. 11790, U.S.A.

Abstract—High-resolution (0.1 cm^{-1}) measurements have been performed on several CO_2-broadened lines in the fundamentals of HCl^{35} and HCl^{37}. Line intensities, half-widths and shapes have been determined at room temperature. Half-widths in HCl–CO_2 and HF–CO_2 collisions have been computed for several temperatures employing Anderson's theory. The measured shapes of HCl lines broadened by CO_2 are described by a semi-empirical super-Lorentzian line shape, given by

$$k_\nu = \frac{S}{\pi\gamma}\left(\frac{\eta}{2}\sin\frac{\pi}{\eta}\right)\left[\left(\frac{|\nu-\nu_0|}{\gamma}\right)^{\eta}+1\right]^{-1} \tag{1}$$

with $\eta = 1.75$. The curve-of-growth for this line shape has been derived in terms of a function similar to the Ladenburg–Reiche function. Absorption between $R(0)$ and $P(1)$ is affected by the appearance of several pressure-induced Q-branch lines, at the pressures from one to ten atmospheres used in the present study.

INTRODUCTION

THE WORK reported in this paper has been prompted by the recent discovery[1] of traces of HCl and HF in the atmosphere of Venus, which is composed predominantly of CO_2. Both HCl and HF are present in such trace amounts (partial pressures of the order of 10^{-4} and 10^{-6} torr[1]) as to make them optically thin. Line-width information may not really be required to estimate their abundances. However, since the rotational lines in both HCl and HF bands are well separated and, hence, well resolved, they would seem singularly attractive for studying line-formation in the Cytherean atmosphere. A thorough understanding of the purely absorbing profiles of HCl (and HF) lines in CO_2 atmospheres should provide an important first look at the more complex line-shape studies in a scattering–absorbing atmosphere. Furthermore, planetary transmission studies, besides the Cytherean case, require line-shape information for dipolar molecules (H_2O, NH_3, HCl, H_2S, etc.) in atmospheres that are composed predominantly of quadrupolar molecules (N_2, H_2, CO_2, etc.). Hence, an extensive experimental study of collision-broadened line shapes in dipole–quadrupole collisions may have practical, as well as academic, utility.

* Supported by NASA under Grant No. NGR-33-015-139.

† Present address: Department of Physics and Astronomy, The University of Tennessee, Knoxville, Tenn. 37916, U.S.A.

Two suitable molecules for study are HCl and CO_2 since both are linear molecules; HCl is strongly polar while CO_2 is a large quadrupole.

The work which we report here is similar to that of BENEDICT *et al.*[2]

EXPERIMENTAL DETAILS

We have employed an Ebert-mounted grating spectrophotometer with a resolution of approximately 0.1 cm^{-1} to study the spectra of HCl^{35} and HCl^{37} between 2700 and 3100 cm^{-1}. Six absorption cells have been used. Three glass cells of lengths equal to 0.04, 1 and 10 cm were sealed with infrared-grade fused-silica ("Infrasil") windows. Calcium fluoride windows were used on a 2 cm long glass-bodied absorption cell and a meter long White cell. A 5 cm long stainless steel high-pressure cell was also used with fused-silica windows. The cell length of the smallest cell was calibrated using well-established lines in the CO fundamental.[3] Mixtures of HCl and CO_2 were prepared with technical grade (99 per cent) HCl and Coleman Instrument grade (99.99 per cent pure) CO_2. The gases were allowed to mix for several days in stainless-steel cylinders. The concentration of HCl was determined by measuring the intensities of several lines and calibrating them against the intensities obtained using pure HCl. Each gas mixture was used for at least a week; no appreciable loss in the concentration of HCl was observed. Three ratios, equal to 0.03, 0.075 and 0.165, of the partial pressure of HCl to the total pressure were used. The spectra were taken at a scanning rate of 0.15 cm^{-1}/min with a time constant of 8 sec and with 1 per cent noise.

LINE INTENSITIES IN THE FUNDAMENTALS OF HCl^{35} AND HCl^{37}

At least three sets of published data[2,4,5] are available for the line intensities in the fundamental bands of HCl^{35} and HCl^{37}. Two sets[2,4] are in wide disagreement with each other. Since line intensity is an important parameter in determining line shape, we have remeasured the intensities of HCl^{35} lines using pure HCl samples and the 0.04 cm cell. At this path-length and pressures of 1 and 2 atm, practically no overlapping was observed between the lines of isotopic pairs at a spectral resolution of 0.1 cm^{-1}. Our data shown in Table 1 are the results of independent measurements made on the two isotopic lines. The estimated accuracy of our line-intensity measurements is about 5 per cent.

MEASUREMENT AND COMPUTATION OF CO_2-BROADENED HALF-WIDTHS

Line widths have been measured using a "curve-of-growth" procedure, which was coupled with an iterative process of matching the observed and computed transmission contours. The curve-of-growth measurements were carried out at total pressures of 1 and 2 atm. Before the exact form of the line shape was recognized the Ladenburg–Reiche curve-of-growth was used. These estimates were then revised according to the modified curve of growth (see Appendix) for the super-Lorentzian profile which best fitted the experimental data. The resulting half-widths were not only consistent with the new curve-of-growth, but also matched the data obtained under conditions when direct line-width measurements were possible.

TABLE 1. LINE INTENSITIES, S_m (cm^{-2} atm^{-1}), IN THE FUNDAMENTAL BANDS OF HCl^{35} AND HCl^{37} AT 295°K

Line	S_m (cm^{-2} atm^{-1})							
	HCl^{35}				HCl^{37}			
	This study	Ref. (2)	Ref. (4)	Ref. (5)	This study	Ref. (2)	Ref. (4)	Ref. (5)
P(8)	1.44	—	1.41	1.32	0.48	0.428	0.463	0.433
P(7)	2.59	2.46	2.70	2.40	0.90	0.918	0.883	—
P(6)	4.52	4.16	4.54	4.17	1.54	1.44	1.48	1.34
P(5)	6.73	5.79	6.72	—	2.18	1.93	2.19	2.04
P(4)	9.00	7.58	8.91	–	2.93	2.48	2.90	2.73
P(3)	9.41	8.49	9.32	—	3.02	3.10	3.04	2.79
P(2)	8.20	7.46	8.16	—	2.72	2.54	2.66	2.54
P(1)	5.00	4.56	4.96	—	1.61	1.54	1.61	1.55
R(0)	5.25	4.71		4.90	1.72	1.61		1.61
R(1)	8.98	8.52		—	2.90	2.95		2.96
R(2)	10.20	9.61		—	3.09	3.13		3.42
R(3)	10.00	9.43		—	3.40	3.46		3.25
R(4)	7.92	7.65		—	2.61	2.47		2.71
R(5)	6.60	5.98		—	2.20	2.03		1.98
R(6)	4.24	3.69		3.74	1.40	1.40		1.25
R(7)	2.10	2.11		2.12	0.68	0.661		0.701
R(8)	1.07	1.07		1.09	0.44	0.418		0.359
R(9)	0.480	0.481		0.476	0.17	—		0.156
R(10)	0.194	—		0.197	0.067	—		0.654
R(11)	0.0625	—		0.0689	0.022	—		0.0220

$S_{band} = 140 \pm 10\ cm^{-2}\ atm^{-1}$

The measured half-widths in HCl–CO_2 collisions are compared in Fig. 1 with the data of BABROV *et al.*[4] together with a computation using Anderson–Tsao–Curnutte theory.[7] In our studies, no distinction has been drawn between the half-widths of HCl^{35} and HCl^{37} lines, or of the *P* and *R* branch lines with the same *m*, since they were nearly equal. The data of Babrov *et al.* are for the first eight lines in the *P* branch, whereas our data cover both *P* and *R* branches up to *R*(12). Half-widths computed at 200 and 250°K, at which no experimental data are currently available, are also shown in Fig. 1. Half-width computations in HF–CO_2 collisions, which are practically identical to those involving HCl–CO_2 collisions, were also made using Anderson's theory at 200, 250 and 295°K. Our results and a comparison with the experimental data of SHAW and LOVELL[14] are shown in Fig. 2. The various molecular constants that have entered the half-width calculations are given in Table 2.

In the notation used in Table 2, μ is the dipole moment, θ is the quadrupole moment, $\alpha_{\parallel}$ and $\alpha_{\perp}$ are, respectively, the parallel and perpendicular components of polarizability, ε is the ionization potential, $B_{[0]}$ the ground state rotational constant and σ_{kin} refers to the collision diameter according to kinetic theory.

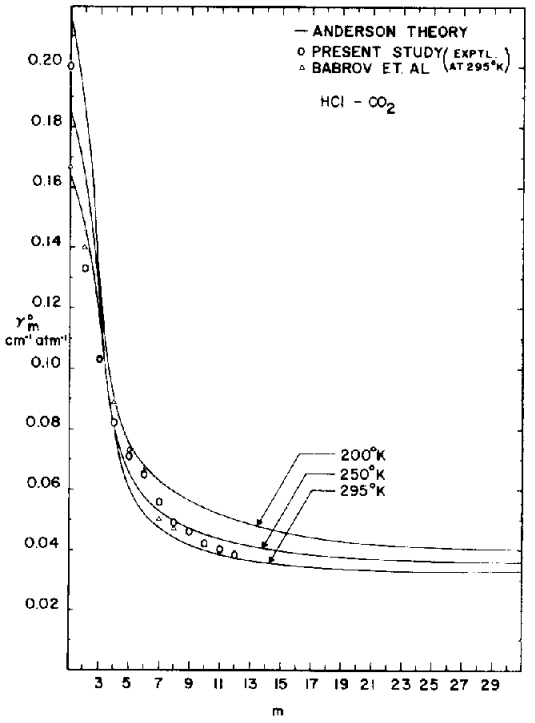

FIG. 1. CO_2-broadened half-widths of HCl lines at 200, 250 and 295°K. The experimental data, at room temperature, for lines in the fundamentals of HCl^{35} and HCl^{37} are shown by circles and triangles.[4]

MEASUREMENT OF LINE SHAPES

The results shown in Figs. 3–7 are typical of our line-shape measurements in the HCl fundamental. Such data were obtained with a line-width to spectral slit-width ratio of 5 to 1 or greater. Hence, slit-function corrections were found to be quite negligible. This fact

TABLE 2. INDIVIDUAL MOLECULAR CONSTANTS

	HCl	HF	CO_2	Ref.
μ (10^{-18} e.s.u. cm)	1.07	1.74	0	8
θ (10^{-26} e.s.u. cm^2)	3.8	2.6	4.3	8
$\alpha_{\parallel}$ (10^{-25} cm^3)	31.3	39.6	40.6	9
$\alpha_{\perp}$ (10^{-25} cm^3)	23.9	17.2	19.5	9
ε (10^{-11} ergs)	2.211	2.836	2.307	10
$B_{[0]}$ (cm^{-1})	10.4	20.6	0.389	11
σ_{kin} (Å)	3.305	3.1	4.07	9

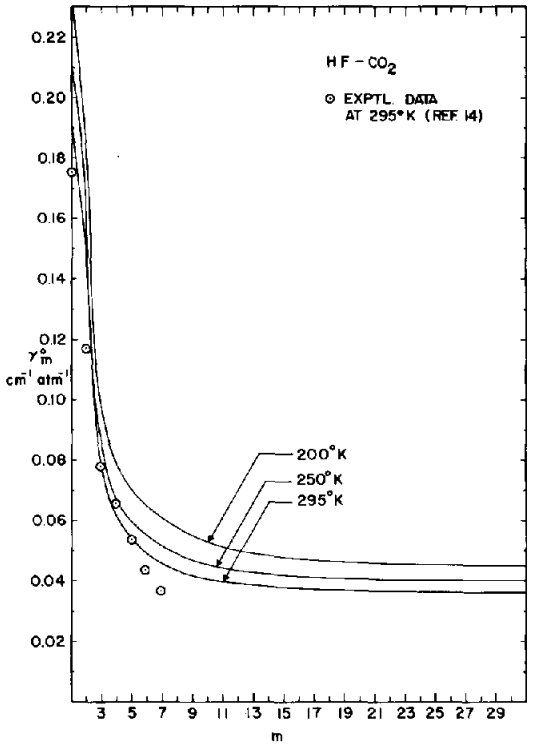

FIG. 2. CO_2-broadened half-widths of HF lines computed at 200, 250 and 295°K using Anderson–Tsao–Curnutte theory. Circles represent the experimental data of SHAW and LOVELL[14] at 295°K.

was verified by a computer program that was carried out for Lorentz profiles and super-Lorentz profiles including the distortion due to slit-function corrections. In this program the computed transmission at each frequency accounts for the absorption due to three isotopic pairs, i.e. six lines, on either side of its wave number location, making a total of twelve lines at each wave number. The solid curves in Figs. 3–7 are the results of such computations for the super-Lorentz profile given by the following expression for the absorption coefficient:

$$k_\nu = \frac{S}{\pi\gamma}\left(\frac{\eta}{2}\sin\frac{\pi}{\eta}\right)\left[\left(\frac{|\nu-\nu_0|}{\gamma}\right)^\eta + 1\right]^{-1} \tag{1}$$

with $\eta = 1.75$. (See Appendix for a detailed discussion on how we arrive at this expression.) The dotted lines in Figs. 5 and 6 are for Lorentz lines, for which

$$k_\nu = \frac{S}{\pi\gamma}\left[\left(\frac{\nu-\nu_0}{\gamma}\right)^2 + 1\right]^{-1}. \tag{2}$$

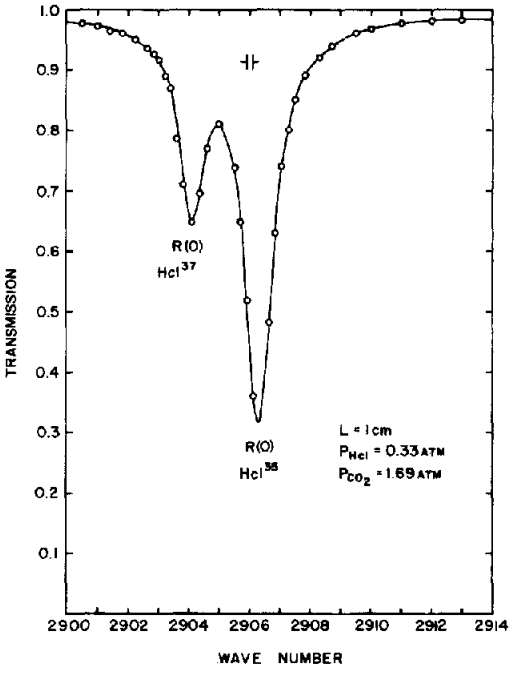

FIG. 3. Comparison of measured and super-Lorentz [equation (1)] profiles of spectral transmission of CO_2-broadened lines $R(0)$ in the fundamentals of HCl^{35} and HCl^{37}. $T = 295°K$.

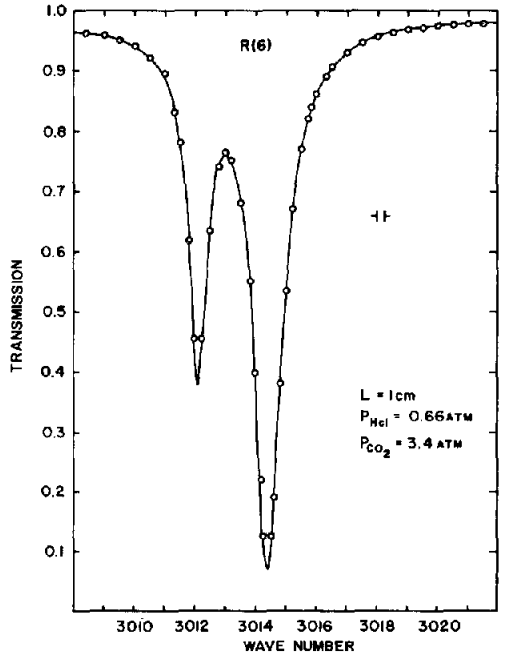

FIG. 4. Comparison of measured and super-Lorentz [equation (1)] profiles of spectral transmission of CO_2-broadened lines $R(6)$ in the fundamentals of HCl^{35} and HCl^{37}. $T = 295°K$.

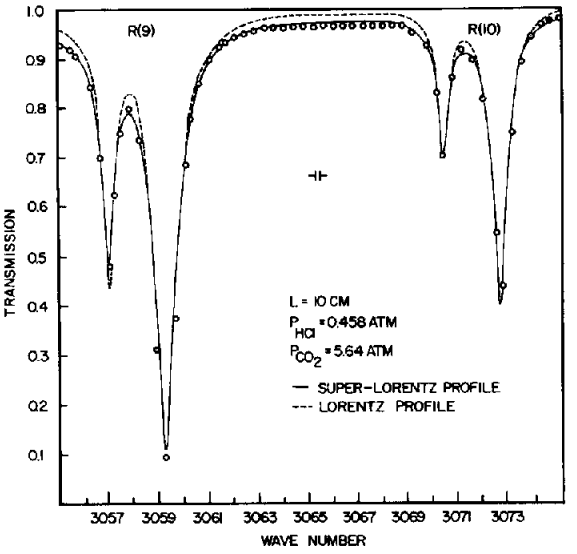

FIG. 5. Comparison of measured and theoretical profiles of spectral transmission of CO_2-broadened lines $R(9)$ and $R(10)$ in the fundamentals of HCl^{35} and HCl^{37}. The solid curve represents super-Lorentz profile [equation (1)] and the dotted curve is for the Lorentz profile [equation (2)]. $T = 295°K$.

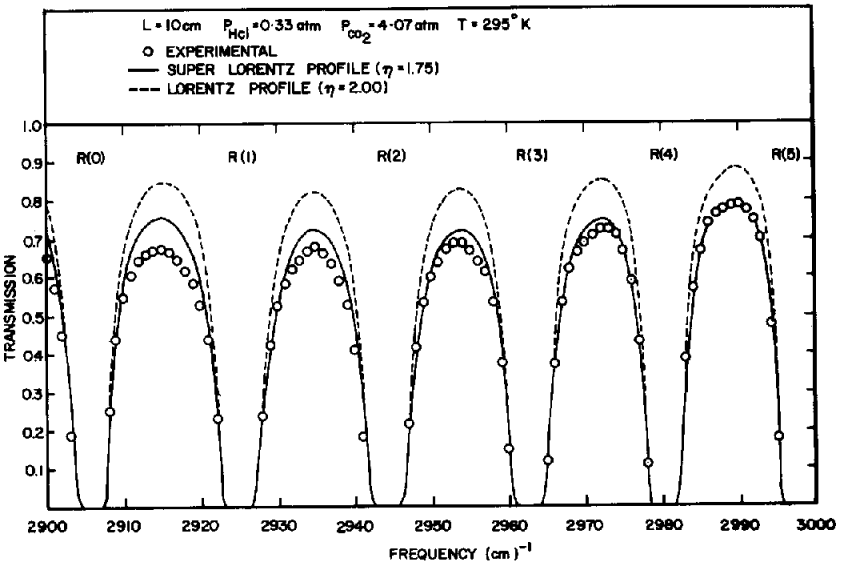

FIG. 6. Comparison of measured, Lorentz (dotted) and super-Lorentz [equation (1), solid curve] profiles of spectral transmission in the fundamentals of HCl^{35} and HCl^{37}, between 2900 and 3000 cm^{-1}, at 295°K.

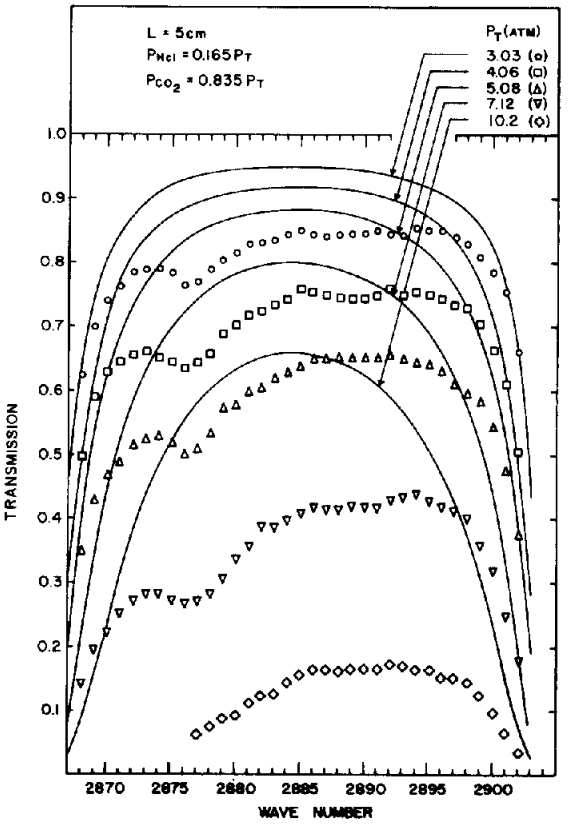

FIG. 7. Comparison of measured and super-Lorentz [equation (1)] profiles of spectral transmission in the zero gaps of the fundamentals of HCl^{35} and HCl^{37}, at 295°K.

MEASUREMENT AND EMPIRICAL DETERMINATION OF LINE-SHAPE PARAMETERS FOR THE PRESSURE-INDUCED Q-BRANCH

We see, from the data shown in Fig. 7, a pressure induced Q-branch in the "zero gap" between the lines $P(1)$ and $R(0)$. Influence of the Q-branch can also be observed, though much less directly, in Fig. 6, as it appears in the form of enhanced absorption in the troughs between the R-branch lines with $J < 4$. From Figs. 3–5 and from data that were taken under similar conditions for the rest of the R-branch lines, it is clear that the super-Lorentz contour given by equation (1) describes the line shape quite accurately. The agreement between the theoretical and the measured line contours is excellent in two conspicuous cases. In the case of low J-lines shown in Figs. 3 and 4, the path length is too small to exhibit any influence due to the wing of the Q-branch. As pointed out earlier, the contributions from neighboring lines (excepting the Q-branch) have already been taken into account in drawing the theoretical contours. In the second case (shown in Fig. 5) the lines under consideration are nearly 200 cm^{-1} away from the central Q-branch, so that, even for a path length of 10 cm and a total pressure of 6.1 atm, we see little evidence of Q-branch contribution to the local absorption. Thus, once we accept the line profile as given by

equation (1) as a true representation of the shape of all the R-branch lines, we may attribute the striking difference between the measured and the computed transmission shown in Figs. 6 and 7 to the absorption by the Q-branch. This is obvious in Fig. 7 and is less so in Fig. 6. However, we note in Fig. 6 that the excess in the measured absorption over the computed value in the troughs between the lines is increasing as we approach the location of the Q-branch. Therefore, if we plot the difference between the measured and the computed transmission as a function of wave number, we obtain the absorption contours for the Q-branch such as those shown in Figs. 8 and 10. The absorption coefficient referred to in Fig. 8 is defined by the relation

$$k_\nu = (pl)^{-1} \log_e [\tau_{\nu,\text{expt}}/\tau_{\nu,PR}], \tag{3}$$

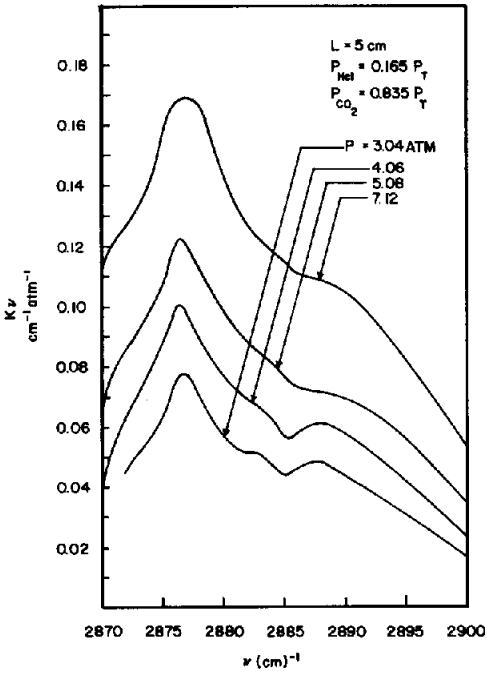

FIG. 8. Apparent spectral absorption coefficients for pressure-induced Q-branches in the fundamentals of HCl^{35} and HCl^{37} at 295°K.

where $\tau_{\nu,\text{expt}}$ and $\tau_{\nu,PR}$ are, respectively, the experimental transmission and the computed non-Lorentz transmission which accounts for only the P and R branch lines; p is the partial pressure of HCl and l is the cell length.

In Fig. 9 we show the local (spectral) absorption coefficients at five frequencies in the Q-branch, as obtained from the data in Fig. 8 and plotted against the total pressure. The linear dependence of k_ν on total pressure, which is a constant multiple of the partial pressure of the perturbing gas (CO_2 in this case), is a well known characteristic of pressure-induced absorption. Hence it is more useful to work with the quantity k_ν/p_T which is plotted in

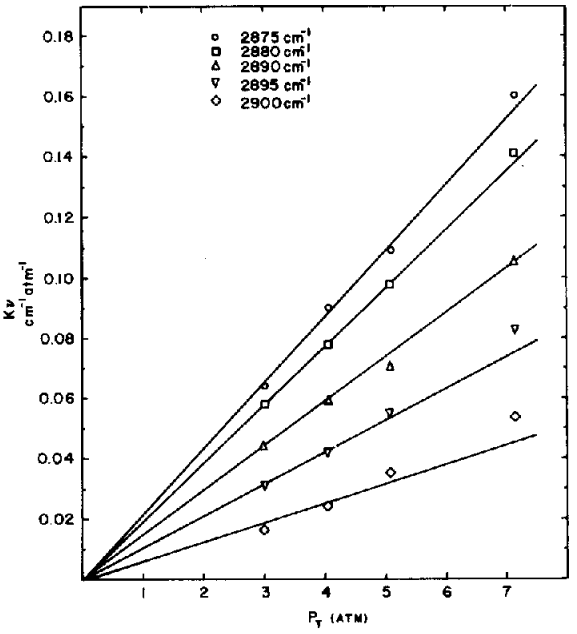

FIG. 9. Variation of the apparent spectral absorption coefficients for pressure-induced Q-branches in the fundamentals of HCl^{35} and HCl^{37} at several selected frequencies. $T = 295°K$.

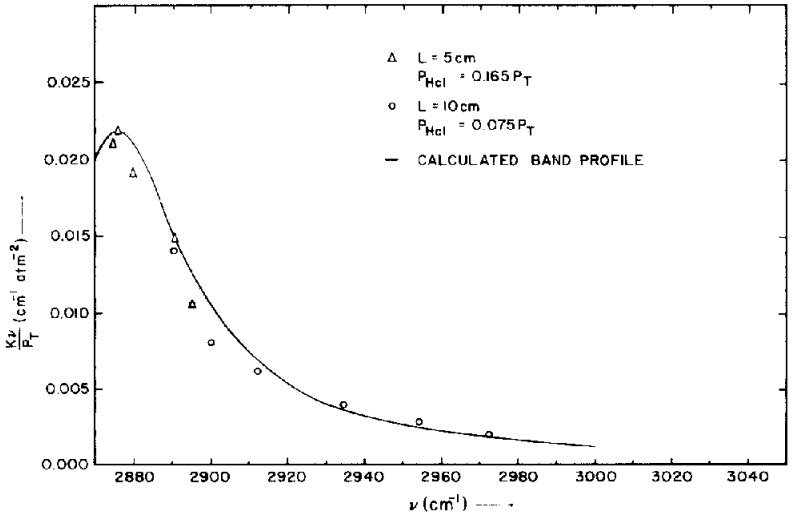

FIG. 10. Comparison of measured and semi-empirical contours of the pressure-induced Q-branch at 295°K. The ordinate identifies the spectral absorption coefficient normalized to one atmosphere of total pressure.

Fig. 10 as a function of frequency. The experimental data beyond 2900 cm^{-1} are obtained from Fig. 6 by using equation (3). From spectral absorption coefficient data such as those shown in Fig. 10, it should be possible, at least in a semi-empirical manner, to arrive at some estimates for the strengths and widths as well as shapes of the individual (though thoroughly blended) lines of the pressure-induced Q-branch. A first and approximate set of conclusions based upon such procedure is discussed in the last section.

CONCLUSIONS

We focus our attention first at the line intensities given in Table 1. The most striking feature is the agreement among all measurements listed in the table for the R-branch lines with $m \geq 8$, for both HCl^{35} and HCl^{37}. Thus one may safely say that the intensities of these lines appear to be established. Intensities of these lines are what we have actually used in determining the composition of our HCl–CO_2 mixtures. The intensity data for lines in the R-branch with $m < 8$ and of all the lines in the P branch obtained by using the samples (mixtures) thus calibrated were consistent with the data obtained using pure HCl samples. They are also in excellent agreement with the data of BABROV *et al.*[4] for the lines in the P-branch. Thus, we believe the intensity estimates of BENEDICT *et al.*[2] and of TOTH *et al.*[5] may be in error. We are unable to locate the possible sources of error.

Our estimate for the total integrated intensity of the entire band is arrived at by adding the intensities of all of the lines we have measured. P-branch lines with $m > 8$ and R-branch lines with $m > 12$, which have not been included in Table 1, might contribute about 2 per cent to the total intensity.[2] Hence, our estimate should be accurate within the 5 per cent error limits we have already quoted for the line intensity data and the additional error of 2 per cent we have just mentioned. It is interesting to observe that our result is precisely the "lower limit" obtained by PENNER and WEBER[6] using an absorption cell of length equal to 0.5 and pure HCl at pressures up to 20 atm. Their measurements for larger path-lengths (see Fig. 5 of Ref. 6) asymptotically approach this limit as the product pl goes to zero. Thus, a reinterpretation of their data may be a plausible means of resolving a long-sustained "controversy" between the low "high-resolution estimates" based upon line-intensity measurements (Refs. 2, 4, 5 and this study) and the high "low-resolution estimates" of PENNER and WEBER[6] (and of others mentioned in Ref. 6).

By means of data such as those shown in Figs. 3–6, we are convinced that the semi-empirical line shape given by equation (1) is an accurate fit of the experimental line contours. It is a well-known result in the statistical (or quasi-static) line-broadening theory[2,12] that the shape of spectral lines subject to a statistical (or quasi-static) perturbation by intermolecular potentials, which vary with intermolecular distance as $\pm cr^{-n}$, is given by

$$k_\nu \sim (\nu - \nu_0)^{-(n+3)/n}$$

at frequencies far from the line center ν_0. In the case of HCl–CO_2 collisions the dominant interaction is due to dipole–quadrupole forces for which $n = 4$. Thus, we have

$$\eta = (n+3)/n = 1.75,$$

which is precisely the value used by us. The line shapes given by statistical theories have two inherent drawbacks.[12] Firstly, the profiles are not symmetrical about the line center unless $\eta = 2$, which is the case for resonant dipole–dipole forces. Secondly, the theory fails

for frequencies near the line-center. Thus we find it necessary to "improvise" a little and (i) artificially make the shape symmetrical by taking only the absolute value of $(\nu - \nu_0)$ and (ii) introduce the second term (equal to unity) in the denominator of equation (1). The first step is dictated by the apparent symmetrical shape observed experimentally in the infrared and the second step is necessary to preserve the central portion of a line. The actual form of the second term in the denominator of equation (1) is prompted by the fact that for $\eta = 2$, we recover the Lorentz line-shape. The justification for developing this particular algebraic form of the profile, however, rests quite heavily upon the remarkable success with which it describes the experimental shape of an entire line. (See Figs. 3–5.)

In Figs. 1 and 2, we show comparison of experimental half-widths with those computed using Anderson's theory. The theory seems to match fairly well the experimental data (Fig. 1) for HCl lines over a wide range of values of the quantum number m excepting the "hump" portion between $m = 5$ and $m = 8$. In Fig. 2 for HF–CO_2 collisions, we note good agreement between the theoretical half-widths and the data of SHAW and LOVELL[14] for $m < 6$. Further experimental work on CO_2-broadened HF lines, especially on lines with $m \geq 7$, is clearly warranted to establish the trend of the γ_m^0 vs. m curves for large values of m.

Anderson's theory is essentially an impact-broadening theory which necessarily requires the time spent by the molecules in a collision, which interrupts the radiation, to be negligible in comparison with the mean time between the collisions. This assumption leads to a generalized Lorentz line shape that takes line-shift also into account. On the other hand, a statistical broadening theory is built upon the exact opposite viewpoint. It requires that the time spent in a collision be comparable with the mean time between collisions (hence, the label "quasi-static"). It is also implicit in the basic framework of the statistical theory that the collisions are no longer binary as in the case of impact-broadening theories. The utter inadequacy of the Lorentz lineshape in HCl–CO_2 collisions observed in the present study makes it difficult to conceive of the collisions as impact phenomena. Therefore, we can only view upon the success with which one could apply Anderson's theory to HCl–CO_2 collisions as to imply that the strength of the Anderson–Tsao–Curnutte approach lies not so much in the basic assumptions discussed above, but in the detailed, and fairly effective, manner in which the important intermolecular interactions are taken into account by the theoretical model.

The line shape introduced in this paper for dipole–quadrupole collisions could have conceivable application in similar cases of broadening. For example, in NH_3–H_2, H_2O–N_2, H_2O–CO_2, H_2S–H_2, HF–CO_2, etc. In the case of NH_3–H_2 collisions some preliminary studies seem to show some evidence in this direction. These and other line-shape studies (involving H_2O–N_2 and H_2O–CO_2) will be published at a later date.

Finally, we wish to present semi-empirical estimates for the pressure-induced Q-branches of HCl^{35} and HCl^{37}. We make the following salient assumptions:

(a) The relative intensities of lines with different J's but belonging to the same isotopic species are proportional to the Boltzmann factors of the rotational levels of the unperturbed molecule.

(b) The frequency separations between HCl^{35} and HCl^{37} lines are the same as in the P- and R-branches.

(c) The measured line intensities of the two species of each isotopic pair bear the same ratio as do their abundances, i.e. a ratio of $HCl^{35}:HCl^{37} = 3.07:1$.

(d) The transition probabilities for the Q-branch lines are the quadrupole transition probabilities for $J = 0$, i.e.

$$Q(J, J) = \frac{J(J+1)}{(2J-1)(2J+3)}.$$

(e) The Q-branch lines have the same shape as the P- and R-branch lines do, with the exception that their long wave-length wings are diminished by a Boltzmann factor which is a characteristic of pressure-induced absorption.[15] The half-widths are nearly 200 times larger than the half-widths of the lines of the P- and R-branches as is usually the case with collision-induced lines. We further assume that the lines have nearly the same J-dependence as the P- and R-branch lines.

(f) The locations of the Q-branch lines are uniformly shifted by approximately 2 cm^{-1} (experimental fact) in the case of perturbation by CO_2 molecules from the theoretical line positions for an unperturbed molecule. Some further evidence for the large shifts in the pressure-induced Q-branch lines (different for different perturbers) may be found in the paper by RANK *et al.*[13]

Under the assumptions (a)–(f), we may now write a semi-empirical expression for the (continuum) absorption coefficient in the Q-branch:

$$\frac{k_\nu}{p_T} = S^0_{(Q)} \frac{\sum_{J=1}^{\infty} Q(J, J) g_J \exp\left[-\frac{hcBJ(J+1)}{kT}\right] \cdot \frac{\chi_J}{\pi\gamma_{J,Q}}\left(\frac{\eta}{2}\sin\frac{\pi}{\eta}\right)\left[\left|\frac{\nu-\nu_J}{\gamma_{J,Q}}\right|^\eta + 1\right]^{-1}}{\sum_{J=1}^{\infty} Q(J, J) g_J \exp\left[-\frac{hcBJ(J+1)}{kT}\right]},$$

where

$$\chi_J = 1 \text{ for } \nu \geq \nu_J, \text{ and } \chi_J = \exp\left[\frac{hc}{kT}(\nu-\nu_J)\right] \quad \text{for } \nu \leq \nu_J.$$

Here B is the rotational constant of the unperturbed HCl molecule, $S^0_{(Q)}$ [cm^{-2} atm^{-2}] is the total integrated intensity of the pressure-induced Q-branch at one atmosphere and T is the temperature (in °K). The constants $S^0_{(Q)}$ and $\gamma^0_{J,Q}$ are determined by fitting the data shown in Fig. 10 with equation (4). Our best estimates for the two parameters are

$$S^0_{(Q)} = 1.5 \pm 0.2\,cm^{-2}\,atm^{-2}$$

and

$$\gamma^0_{J,Q} = 200\,\gamma^0_{P,R}\,cm^{-1}\,atm^{-1}.$$

Acknowledgement—We are indebted to Professor W. S. BENEDICT for his generous comments throughout the course of this investigation.

REFERENCES

1. P. CONNES, J. CONNES, W. S. BENEDICT and L. D. KAPLAN, *Astrophys. J.* **147,** 1230 (1967).
2. W. S. BENEDICT, R. HERMAN, G. E. MOORE and S. SILVERMAN, *Can. J. Phys.* **34,** 850 (1956).
3. W. S. BENEDICT, R. HERMAN, G. E. MOORE and S. SILVERMAN, *Astrophys. J.* **135,** 277 (1962).
4. H. BABROV, G. AMEER and W. BENESCH, *J. chem. Phys.* **33,** 145 (1960).
5. R. A. TOTH, R. H. HUNT and E. K. PLYLER, *J. Molec. Spectrosc.* **35,** 110 (1970).

6. S. S. PENNER and D. WEBER, *J. chem. Phys.* **21,** 644 (1953).
7. P. W. ANDERSON, *Phys. Rev.* **76,** 647 (1949); C. J. TSAO and B. CURNUTTE, *JQSRT* **2,** 41 (1962). See also D. ROBERT, M. GIRAUD and L. GALATRY, *J. chem. Phys.* **51,** 2192 (1969).
8. D. E. STOGRYN and A. P. STOGRYN, *Mol. Phys.* **11,** 371 (1966).
9. J. O. HIRSCHFELDER, C. F. CURTISS and R. B. BIRD, *Molecular Theory of Gases and Liquids*. John Wiley, N.Y. (1954).
10. *Handbook of Chemistry and Physics* (Ed. R. C. WEAST *et al.*), Chemical Rubber Company, Cleveland, Ohio (1969).
11. G. HERZBERG, *Spectra of diatomic molecules*, Van Nostrand, Princeton, N.J. (1950); *Infrared and Raman Spectra*, Van Nostrand, Princeton, N.J. (1945).
12. R. G. BREENE, JR., *The Shift and Shape of Spectral Lines*, Pergamon Press, New York (1961).
13. D. H. RANK, B. S. RAO and T. A. WIGGINS, *J. chem. Phys.* **37,** 2511 (1963); see also the theoretical study of S. BRATOZ and M. L. MARTIN, *J. chem. Phys.* **42,** 1051 (1965).
14. B. M. SHAW and R. J. LOVELL, *J. opt. Soc. Am.* **59,** 1598 (1969).
15. H. L. WELSH and J. L. HUNT, *JQSRT* **3,** 385 (1963); Z. J. KISS and H. L. WELSH, *Can. J. Phys.* **37,** 1249 (1959); D. A. CHISHOLM, J. C. F. MACDONALD, M. F. CRAWFORD and H. L. WELSH, *Phys. Rev.* **88,** 957 (1952).

APPENDIX

In this appendix, we develop the "super-Lorentz" line shape given by equation (1) and the corresponding curve of growth.

We begin by describing the spectral line shape in terms of a spectral absorption coefficient:

$$k_\nu\,(\mathrm{cm}^{-1}\,\mathrm{atm}^{-1}) = S \cdot f(\nu - \nu_0\,;\gamma). \tag{A-1}$$

Here S ($\mathrm{cm}^{-2}\,\mathrm{atm}^{-1}$) is the integrated intensity of the line and $f(\nu-\nu_0\,;\gamma)$ is the "line shape factor" given in terms of the frequency displacement $(\nu-\nu_0)$ from the frequency ν_0 at the line center and γ, the collision-broadened half-width.

We require that the shape factor $f(\nu-\nu_0\,;\gamma)$ exhibit the following essential features:

(i) symmetrical about the central frequency:

$$\therefore \quad f(\nu-\nu_0\,;\gamma) \equiv f(|\nu-\nu_0|\,;\gamma).$$

(ii) normalized such that $\int_{-\infty}^{\infty} k_\nu\,\mathrm{d}(\nu-\nu_0) \equiv S$

$$\therefore \quad \int_{-\infty}^{\infty} f(\nu-\nu_0\,;\gamma)\,\mathrm{d}(\nu-\nu_0) = 2\int_{0}^{\infty} f(|\nu-\nu_0|\,;\gamma)\,\mathrm{d}(\nu-\nu_0) = 1.$$

(iii) the far wings of the line ($|\nu-\nu_0| \gg \gamma$) vary according to the shape given by statistical theory, i.e. $f(\nu-\nu_0) \sim (\nu-\nu_0)^{-\eta}$ where $\eta = (n+3)/n$, with n being the exponent governing the power law dependence ($\pm Cr^{-n}$) of the intermolecular potential upon the intermolecular distance r.

(iv) $f(\nu-\nu_0\,;\gamma)$ be finite at $\nu = \nu_0$, and (v) the form of $f(\nu-\nu_0\,;\gamma)$ be general enough as to include the Lorentz line shape as a particular case. (For resonant dipole–dipole interactions $\eta = 2$, it should lead to the Lorentz line shape.) By letting

$$f(\nu-\nu_0\,;\gamma) = C\left[\left|\frac{\nu-\nu_0}{\gamma}\right|^{\eta} + 1\right], \qquad (1 < \eta \leq 2) \tag{A-2}$$

we satisfy the requirements (i), (iii), (iv) and (v). It would seem that one could use a constant, to be quite general, in place of the factor unity in the denominator. However, it would only lead to a different value for γ which is, in any event, determined experimentally. Thus, the constant being absorbed in the value of γ, the above expression should be quite general indeed. The constant C is evaluated by using the normalization condition (ii). A simple integration leads to the result:

$$C = (\eta/2\pi\gamma)\sin(\pi/\eta) \tag{A-3}$$

Substituting equations (A-2) and (A-3) in equation (A-1) we arrive at equation (1):

$$k_\nu = (S/\pi\gamma)\left(\frac{\eta}{2}\sin\frac{\pi}{2}\right)\left[\left(\frac{|\nu-\nu_0|}{\gamma}\right)^{\eta} + 1\right]^{-1}. \tag{1}$$

For $\eta = 2$, equation (1) reduces to the Lorentz line shape. Thus, condition (v) is also met.

Now, we proceed to determine the curve of growth of the profile given by equation (1). By definition, the equivalent width of a spectral line is given by

$$W(\mathrm{cm}^{-1}) = \int_{-\infty}^{\infty} [1-\exp(-k_\nu pl)]\, \mathrm{d}(\nu-\nu_0). \tag{A-4}$$

Substituting equation (1) into equation (A-4), we get

$$W(u) = 2\pi\gamma L(u;\eta) \tag{A-5}$$

where

$$L(u;\eta) = \frac{1}{\pi}\int_0^{\infty}\left[1-\exp\left(-\frac{u\eta\sin(\pi/\eta)}{x^\eta+1}\right)\right]\mathrm{d}x \tag{A-6}$$

with

$$u \equiv (Spl)/(2\pi\gamma)$$

and

$$x \equiv |\nu-\nu_0|/\gamma.$$

The integral in equation (A-6) may be evaluated in terms of the confluent hypergeometric function $M(a, b, u)$ (see I. S. GRADSTEYN and I. M. RYZHIK, *Tables of Integrals, Series and Products.* Academic Press, N.Y. (1965), p. 340). We then obtain

$$L(u;\eta) = \frac{u\eta}{\pi}\sin\left(\frac{\pi}{\eta}\right).\ B\left(1-\frac{1}{\eta},\frac{1}{\eta}+1\right)M\left(1-\frac{1}{\eta},\,2,\,-u\eta\sin\left(\frac{\pi}{\eta}\right)\right) \tag{A-7}$$

where $B(m, n)$ is the beta function. Both the beta function and the confluent hypergeometric function are tabulated and the various asymptotic expansions for the latter are known (see, for example, M. ABRAMOWITZ and I. A. STEGUN, *Handbook of Mathematical Functions.* N.B.S. Appl. Math. Series 55 (1964)).

It is clear from the above development that $L(u; 2) \equiv L(u)$, the Ladenburg–Reiche function. It is worthwhile to verify that it is indeed so. In the process of verification, we shall have arrived at an alternate derivation of the function $L(u)$ from that commonly given in textbooks (see S. S. PENNER, *Quantitative Molecular Spectroscopy and Gas Emissivities*, Addison-Wesley, Reading, Massachusetts (1959), pp. 42–44). For $\eta = 2$, equation (A-7) reduces to

$$L(u;2) = uM(1/2,\,2,\,-2u). \tag{A-8}$$

The conventional form of the Ladenburg–Reiche function is

$$L(u) = u\,\mathrm{e}^{-u}[J_0(iu)-iJ_1(iu)]. \tag{A-9}$$

The Bessel functions in equation (A-9) may be written in terms of confluent hypergeometric functions and using equations (13.4.2) and (13.4.3) of Abrahamovitz and Stegun (*loc. cit*) we obtain

$$\begin{aligned} L(u) &= u\left[M(\tfrac{1}{2},1,-2u)+\frac{u}{2}M(\tfrac{3}{2},3,-2u)\right] \\ &= u[M(\tfrac{1}{2},1,-2u)-\tfrac{1}{2}\{M(\tfrac{3}{2},2,-2u)-M(\tfrac{1}{2},2,-2u)\}] \\ &= uM(\tfrac{1}{2},2,-2u). \end{aligned} \tag{A-10}$$

By comparing equation (A-8) with equation (A-10), we note that $L(u; 2)$ is the Ladenburg–Reiche function. We have plotted both $L(u)$ and $L(u; \eta)$ in Fig. A-1 as functions of u (the curves of growth). For small values of u, both the functions approach the linear limit, since this limit is independent of the shape factor and depends only upon S. On the other hand, the large u limits are quite different. The so-called "square root" limit in the case of $L(u)$ is replaced by a $(1/\eta)$-power limit in the case of $L(u; \eta)$. This may also be seen from the asymptotic expansion of $L(u; \eta)$.

For large values of u:

$$L(u;\eta) = \frac{\Gamma(1-1/\eta)}{\pi}\left(u\eta\sin\frac{\pi}{\eta}\right)^{1/\eta}\left[1+O\left(\frac{1}{u\eta}\right)\right], \tag{A-11}$$

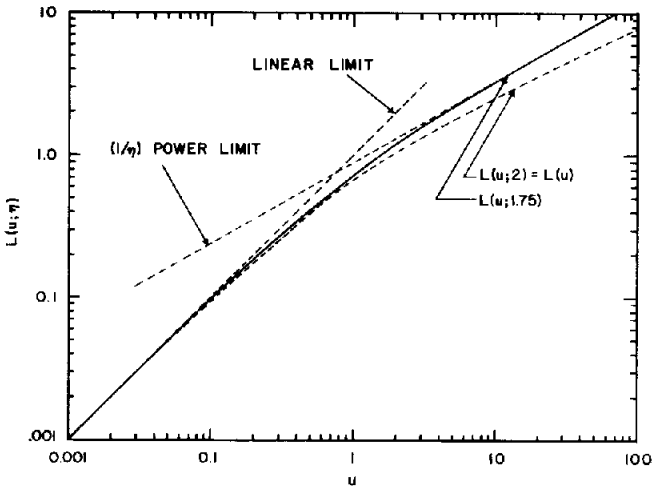

FIG. A-1. Comparison of the "curves of growth" for Lorentz (dotted curve) and super-Lorentz [solid curve—equation (1)] lines.

which, for the special case of $\eta = 2$, reduces to the familiar result

$$L(u;2) = \left(\frac{2u}{\pi}\right)^{1/2}\left[1 + O\left(\frac{1}{2u}\right)\right].$$

It is clear that, for large values of u, the curve of growth for a super Lorentz profile should exceed that of a Lorentz profile, since absorption in the wings of a line determines its equivalent width. It may easily be verified that, since

$$\frac{W(u)}{Spl} = \frac{L(u;\eta)}{u}$$

for an experimentally determined value of $W/(Spl)$, using the super-Lorentz curve of growth would lead to a larger u than for the Ladenburg–Reiche case, and, hence, to a smaller line-width than the Lorentz half-width. It is obvious, from physical grounds, that a line shape having the same integrated intensity must be narrower near the line center than the Lorentz line shape in order to obtain excess absorption in the wings. Such is indeed the case for HCl lines broadened by CO_2.